Attitude dynamics of a dual-spin nanosatellite with a gravitational damper

Anton V. Doroshin, Alexandr V. Eremenko

Samara National Research University Samara, Russia

Abstract

The paper considers a process of a controlled attitude motion of a dual-spin nanosatellite. The main goal of control is to achieve a gravitationally stabilized position in a circular orbit in the shortest possible time. The dual-spin nanosatellite contains a gravitational damper and an internal rotor inside a movable unit. The movable unit can fulfill small controlled inclination relative to the main body of the nanosatellite. The mathematical model of the attitude dynamics of the nanosatellite is built and appropriate control laws are developed. Simulation results confirm the performance of the gravitational damper and efficiency of the control algorithm.

Attitude dynamics of a dual-spin nanosatellite with a gravitational damper

Anton V. Doroshin, Alexandr V. Eremenko

Samara National Research University

Samara, Russia

doran@inbox.ru,   yeryomenko.a@bk.ru

Abstract. **The paper considers the process of the controlled motion of a dual-spin nanosatellite. The main goal of control is to achieve a gravitationally stabilized position in a circular orbit in the shortest possible time. The dual-spin nanosatellite contains a gravitational damper and an internal rotor inside a movable unit. The movable unit can fulfill small controlled inclination relative to the main body of the nanosatellite. The mathematical model of the attitude dynamics of the nanosatellite is built and appropriate control laws are developed. Simulation results confirm the performance of the gravitational damper and efficiency of the control algorithm.**

Keywords: dual-spin nanosatellite, movable unit, gravitational damper, gravitational stabilization, control laws

1. INTRODUCTION

As is known, modern space missions involve the use of nanosatellites with the simplest equipment. In this regard, the development of effective simple methods for controlling and stabilizing the motion of nanosatellites is of great importance.

Among such simple motion control methods, it is advisable to develop methods that use their own mobile functional elements of satellites as control elements and actuators. It is also important to use passive stabilization techniques and natural motion properties to control simple satellites

In this paper, we consider the passive gravitational stabilizing principle, based on the action of the central gravitational field, when the nanosatellite fulfills its own orbital motion in a circular orbit. Then stabilization of the nanosatellite attitude relative to the orbital coordinate system will be possible at reducing the angular velocity of the satellite. It can be provided with the help of the unloading of the angular momentum and kinetic energy by the external torques and internal dampers. The viscous damping was considered in many works. Here we can indicate the pioneer scientific works of F. L. Chernous'ko [1, 2] where the spherical dampers in cavities with liquids were fundamentally studied; also the implementation of this classical scheme was investigated in applied aspects of the spacecraft dynamics in the gravitational field [3-5]; the magnetic version of

the damper was synthesized and described in [6, 7]; and later the spherical inertia geometry of the damper-body was generalized on the three-axial inertia body [8], that allows to use the gravitational torques more effective in the sense of the attitude stabilizing by the gravity gradient.

The motivation for the paper is to develop the nanosatellite scheme, which allows using the natural properties of the dynamics of mechanical systems with movable elements to control the angular motion, and to stabilize the attitude position. In this connection, we will try in this work to construct the appropriate mechanical structure of the nanosatellite (fig.1) containing a main body, a gravitational damper, a movable unit with a internal rotor (fig.1, 2). If we activate the rotor rotation then this construction can be called as a dual-spin nanosatellite. The movable unit can tilt slightly relative to the main body. In this article, to move the movable unit relatively the main body of the nanosatellite, the flexible rods rolled up on small electric motors inside the main body are suggested.

The deflection of the movable unit fulfills in this case by the internal electric motors, which change the length of the rods, and incline the movable unit relatively the main body. In the case of the planar inclination, this scheme of the unit deflection can be implemented on the basis of only two opposite electric motors with simple gears, pulling out flexible toothed belts-rods by the gears rotation on any predefined length.

Of course, this scheme for moving the mobile module is still a purely theoretical development, but it has a very real chance for practical implementation.

This nanosatellite design is justified by the possibility of the variable gyroscopic control torque creation with the help of only one internal rotor, and also by using the gravitational field to provide the attitude orientation and to passive stabilize it by the natural way.

Appropriate control laws for the movable unit angular deflection and for the rotor angular velocity can increase efficiency of the damper action; and then the nanosatellite will achieve the gravitationally stable attitude. Let us find some control laws and investigate some cases of gravitational stabilization using all of indicated dynamical tools in the comparison with each other.

The gravitational damper is the mechanical subsystem that consist of the rigid body with three-axial inertia tensor rigidly fixed in the spherical capsule, which is placed into spherical cavity of the main body of the nanosatellite [8]; and moreover, the space between these spherical surfaces is filled by a viscous liquid medium (e.g., by bismuth, like in [6]).

The action of the gravitational damper is based on the creation of the relative rotation of the internal spherical capsule and the main body of the nanosatellite due to the differences in the inertia moments, and, therefore, due to the differences in the absolute rotational motion in the central gravity field. This relative rotation is realized in a viscose medium and the corresponding liquid friction unloads the angular momentum and the kinetic energy of the attitude motion of the

nanosatellite. This relative rotation stops when booth bodies (the main body of the satellite and the body-damper) achieve gravitational equilibrium position on the orbit. These positions are target orientation positions.

The inequality inertia moments of the internal damper-body represent the main principal difference of the mechanical and mathematical models of the gravitational damper from the classical models. The classical gravitational damper represents the spherical rigid body with the spherical inertia tensor also called as the model of M.A. Lavrentiev [1-5]. This spherical symmetry of the inertia tensor significantly limits the possibility of using different autonomous satellite equipment, instead of a sphere, in the role of the internal damper-body. And, moreover, the body with the spherical tensor inertia always has the stabilized gravitational position, and, therefore, the central gravity field does not include the damper rotation, that also limits the efficiency of the damper.

2. Mechanical model

The mechanical model of the nanosatellite is depicted in Figure 1. In our research we will assume, that the relative angular displacements of the movable unit are small. These deflections do not change the position of the center of mass relative to the main body. In addition, we assume that the gravitational damper is placed exactly in the nanosatellite center of mass. The angular deflections of the movable unit are controlled by the control systems with flexible rods of variable length [9, 10].

We will use the following coordinate systems, where points C_i correspond to centers of mass of bodies, and point C is the center of mass of complete nanosatellite:

- CXYZ – the orbital coordinate system located at the center of mass of the nanosatellite (the axis CZ is directed from the gravity center to the orbital position of the center of mass of the nanosatellite, the axis CY is orthogonal to the orbital plane and CX represents the third right axis);
- $C_1 x_1 y_1 z_1$ are the main central axes of inertia of the main body;
- $C_2 x_2 y_2 z_2$ are the main central axes of inertia of the gravitational damper ($C_2 \equiv C$);
- $C_3 x_3 y_3 z_3$ are the main central axes of inertia of the movable unit;
- $C_4 x_4 y_4 z_4$ are the main central axes of inertia of the rotor;
- $C x_i y_i z_i$ has the origin in the center of mass of the complete satellite and has parallel axes to axes $C_i x_i y_i z_i$.
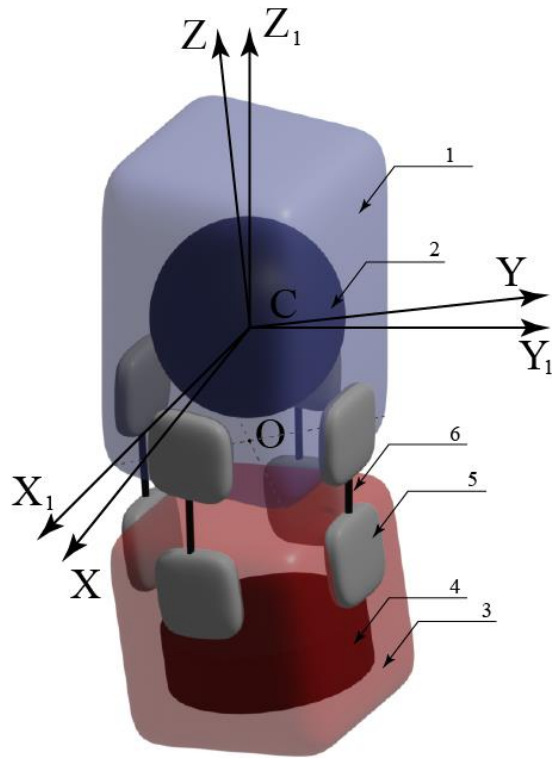
Figure 1 – the nanosatellite construction:

1 – the main body, 2 – the gravitational damper, 3 – the movable unit, 4 – the internal rotor, 5 - flexible rods control system, 6 - flexible rods.
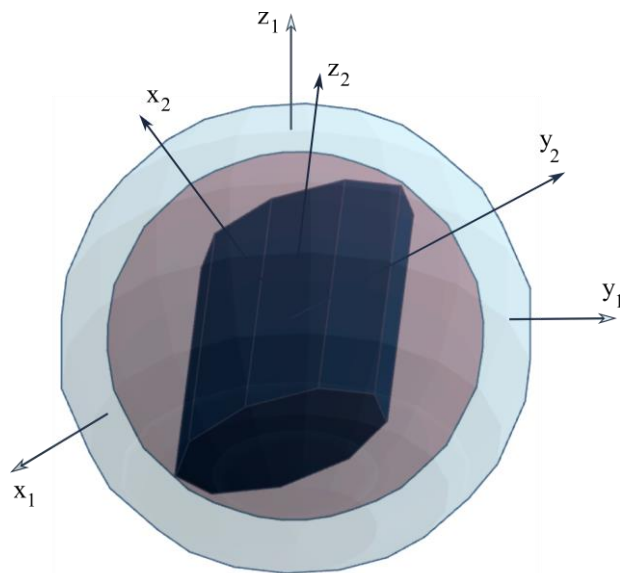

Figure 2 – The internal gravitational damper:

Inside the spherical shell with the viscous medium, there is the inner spherical capsule contained with rigidly fixed triaxial body (some autonomous nanosatellite equipment).

For the purpose of explaining the mechanical structure of the system and damper device, it is ought to shortly remind the natural tendency of the rigid body in the central gravity to receive the so-called "stable gravitational position". As it is known, the ellipsoid of inertia will be placed in the orbital reference frame in such way, that the axis of the minimum inertia moment will correspond to the "longitudinal" axis OZ, connecting the gravity center with the center of mass on the orbit; the intermedium axis of inertia coincides with the axis OX; and the maximum inertia axis of the inertia ellipsoid will be directed along the normal to the orbit plane OY. It is exactly as shown in the picture (fig.3).
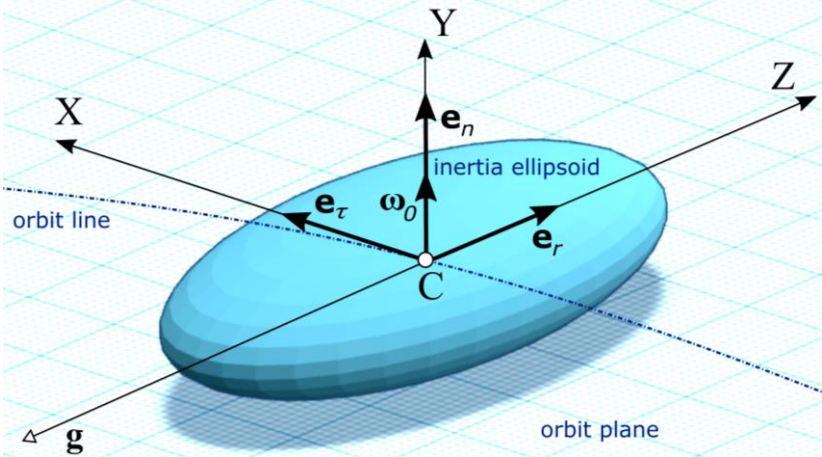

Figure 3 – The gravitational stable position (ω_0 – is the orbital angular velocity)

According to this gravitational property, at the presence of internal dissipation properties in the system, the rigid bodies of the system will independently try to gradually proceed into stable gravitational positions in the orbital axes. Since the inertial properties of the bodies are different, they will make unequal evolutions of angular motion on the transition to the stable gravitational positions. Therefore the bodies will have relative motion and create friction in the contact of their surfaces, i.e. the relative angular motion of the bodies will create the dissipative friction inside the spherical shell with the viscous medium. The resulting dissipation of the kinetic energy allows the bodies of the system to gradually reach their stable positions in the central gravity field. This is the functional principle of the gravity damper, which clarifies its mechanical structure and design (fig.2).

Now let us assume some of the following conditions of motions of the mechanical system bodies. The movable unit is placed on the flexible rods rolled up on small electric motors inside the main body; and, therefore, these internal electric motors can change the length of the rods, and can move the movable unit. In our consideration, the movable unit can fulfill only planar deflections on the small angle α about the axis C_3x_3, which remains always parallel to the axis C_1x_1 (the angle α is the planar angle between the axis C_3z_3 and the axis C_1z_1, or, that is the same, it is the angle between

Cz$_3$ and the axis Cz$_1$,). Moreover, the center of mass C$_3$ of the movable unit always lies on the axis C$_1$z$_1$. The rotor rotates around the axis C$_4$z$_4$, which always coinsides with the axis C$_3$z$_3$ of the movable unit, and, moreover, the center of mass C$_4$ of the rotor and the center of mass of the movable unit C$_3$ are also coincide (C$_3$≡C$_4$). The damper body is rigidly connected to the inner sphere. The damper body has threeaxial inertia tensor, and the center of mass of the damper body coinsides with the geometrical center of the inner sphere. The inner sphere spherically rotates with liquid friction around its own center inside the outer sphere, fixed in the main body. The center of mass of the damper body coinsides with the center of mass of the complete mechanical system (in other words, the center of mass of the subsystem of the nanosatellite without the damper body coinsides with the center of mass of the damper body; and both centers of mass therefore coinside with the center of mass of the complete system).

3.   MATHEMATICAL MODEL

Assume that the movable unit on the flexible rods can make angular turns α around direction of the axis C$_3$x$_3$ relative to the main body with saving the center of mass of movable unit C$_3$ on the axis Cz$_1$ with the constant distance CC$_3$. This assumption means that the movable unit was extended relative the main body to a certain distance by parallel extension of the rods, and after that it makes small planar turns around its own center of mass due to synchronous reciprocal movements of the rods. These planar angular displacements of the movable unit around its own center of mass can be fulfilled by the corresponding change of the flexible rods' length, rolled up on small internal electric motors controlled by the control system of the nanosatellite. The rotor inside the movable unit rotates around the axis C$_3$z$_3$ by the angle γ relatively the movable unit, and, moreover, the center of mass of the rotor C$_4$ always coincides with the center of mass of the movable unit C$_3$. We will also assume that the gravitational damper is located in the main body in such a way that its center of mass coincides with the center of mass of the satellite after it is brought into working condition (after the initial parallel extension of the module on the rods). This allows us to consider that the centers of mass of the satellite in the operating regime and the damper body always coincide.

The damper-body affects the dynamics of the nanosatellite only through the viscous friction torque. In these assumptions, we can write the dynamical equations of our mechanical system on the basis of the law of the angular momentum changing:

$$\frac{d\mathbf{K}}{dt} + \mathbf{\omega}_1 \times \mathbf{K} = \mathbf{M}_b + \mathbf{M}_{gb};$$

$$\frac{d\mathbf{K}_2}{dt} + \mathbf{\omega}_2 \times \mathbf{K}_2 = \mathbf{M}_d + \mathbf{M}_{gd};$$

(1)

where $\mathbf{K}$ is the angular momentum of the complete nanosatellite without the damper-body, $\mathbf{K}_2$ is the angular momentum of the damper-body, $\boldsymbol{\omega}_1$ is the absolute angular velocity of the main body of the nanosatellite, $\boldsymbol{\omega}_2$ is the angular velocity of the damper-body, $\mathbf{M}_b$ is the torque of the viscous friction acting on the main body of the nanosatellite from the side of the damper-body, $\mathbf{M}_d$ is the torque of the viscous friction force acting on the damper-body from the side of the main body, $\mathbf{M}_{gb}$ is the gravitational torque acting on the main subsystem (excluding the damper), $\mathbf{M}_{gd}$ is the gravitational torque acting on the damper.

The angular momentum of the complete nanosatellite without the damper in the system $Cx_1y_1z_1$ can be written as follows:

$$\mathbf{K} = \mathbf{K}_1 + \boldsymbol{\delta}_{31}\mathbf{K}_3 + \boldsymbol{\delta}_{41}\mathbf{K}_4 + m_1\mathbf{V}_1 \times \mathbf{R}_1 + (m_3 + m_4)\mathbf{V}_3 \times \mathbf{R}_3, \tag{2}$$

where $\mathbf{K}_1$ is the angular momentum of the main body relative its own center of mass; $\mathbf{K}_3$ is the angular momentum of the movable unit relative its own center of mass; $\mathbf{K}_4$ is the angular momentum of the rotor relative its own center of mass; $\mathbf{V}_1$ - is the linear velocity of the mass center of the main body arising due to the angular motion of the nanosatellite around the common center of mass; $\mathbf{V}_3$ - is the similar linear velocity of the mass center of the movable unit (and also the rotor); $\mathbf{R}_1$ - is the vector of the center of mass of the carrier body relatively the center of mass of the complete nanosatellite; $\mathbf{R}_3$ - is the vector of the center of mass of the movable unit and rotor body relatively the center of mass of the complete nanosatellite; m_1 - is the mass of the carrier body; m_3 - is the mass of the movable unit; m_4 - is the mass of the rotor. Here $\boldsymbol{\delta}_{31}$ is the transition matrix from the $C_3x_3y_3z_3$ coordinate system to the $Cx_1y_1z_1$ coordinate system, and $\boldsymbol{\delta}_{41}$ is the transition matrix from the $C_4x_4y_4z_4$ coordinate system to the $Cx_1y_1z_1$ coordinate system:

$$\boldsymbol{\delta}_{31} = \begin{bmatrix} 1 & 0 & 0 \\ 0 & \cos(\alpha) & \sin(\alpha) \\ 0 & -\sin(\alpha) & \cos(\alpha) \end{bmatrix}; \tag{3}$$

$$\boldsymbol{\delta}_{43} = \begin{bmatrix} \cos(\gamma) & \sin(\gamma) & 0 \\ -\sin(\gamma) & \cos(\gamma) & 0 \\ 0 & 0 & 0 \end{bmatrix}; \tag{4}$$

$$\boldsymbol{\delta}_{41} = [\boldsymbol{\delta}_{31}][\boldsymbol{\delta}_{43}]; \tag{5}$$

where γ is the angle of rotation of the rotor around the axis C_4z_4 (or around the axis C_3z_3, that is the same in our assumptions) relatively the movable unit.

The angular momentums of the system parts around their own centers of mass are:

$$\mathbf{K}_i = \mathbf{I}_i \boldsymbol{\omega}_i, \tag{6}$$

where i - is the part number: 1 - is satellite main body, 2 - is gravitation damper, 3 - is movable unit, 4 - is rotor. Here $\mathbf{I}_i$ – is the tensor of inertia of the body i, $\boldsymbol{\omega}_i$ – is the absolute angular velocity of the body i.

The inertia tensors of bodies are:

$$\mathbf{I}_i = \mathrm{diag}[A_i; \ B_i; \ C_i], \tag{7}$$

where A_i, B_i, C_i are principal central moments of inertia of the bodies.

To define the vectors $\mathbf{R}_i$, let us to involve the point O on the axis z_1 and on the front side of the main body (fig.1) Then we can define the vectors of the centers of mass of the bodies (C_1, C_3, C_4):

$$\mathbf{OC}_1 = \begin{bmatrix} 0 & 0 & l_1 \end{bmatrix}^T;$$
$$\mathbf{OC}_3 = \begin{bmatrix} 0 & 0 & -l_3 \end{bmatrix}^T; \tag{8}$$
$$\mathbf{OC}_4 = \begin{bmatrix} 0 & 0 & -l_4 \end{bmatrix}^T.$$

Here we remind that in our assumptions $\mathbf{OC}_4 = \mathbf{OC}_3$, or, that is the same, $l_4 = l_3$. Then the vector of the center of mass of the subsystem of bodies ##1, 3, and 4 (i.e. without the damper-body) is:

$$\mathbf{R}_{sub} = \frac{m_1}{m_{sub}} \cdot \mathbf{OC}_1 + \frac{m_3}{m_{sub}} \cdot \mathbf{OC}_3 + \frac{m_4}{m_{sub}} \cdot \mathbf{OC}_4, \tag{9}$$

where m_i is the mass of the body #i, and $m_{sub} = m_1 + m_3 + m_4$. Additionally, we remind that the damper-body is placed in the position of the center of mass of subsystem of bodies ##1, 3, and 4 (i.e. in the position $\mathbf{R}_{sub}$). Therefore, the complete system center of mass coincides with the center of mass of the subsystem (9):

$$\mathbf{R}_c = \left(m_{sub} \mathbf{R}_{sub} + m_2 \mathbf{R}_{sub} \right) / \left(m_{sub} + m_2 \right) = \mathbf{R}_{sub}. \tag{10}$$

This fact also confirms the coincidence of the center of mass of complete system with the center of mass of the subsystem of bodies ##1, 3 and 4, and with the center of mass of the damper-body.

Now we can calculate the vectors of centers of mass of bodies relative to the center of mass of complete nanosatellite, taking into account the parallelism of the axes CXYZ and $C_1x_1y_1z_1$:

$$\mathbf{R}_1 = \mathbf{OC}_1 - \mathbf{R}_c; \tag{11}$$

$$\mathbf{R}_3 = \mathbf{OC}_3 - \mathbf{R}_c; \tag{12}$$

$$\mathbf{R}_4 = \mathbf{OC}_4 - \mathbf{R}_c; \tag{13}$$

The linear velocities of the bodies' centers of mass, which arising due to the angular motion of the

nanosatellite around the common center of mass, are fully defined by the angular velocity of the main body:

$$\mathbf{V}_i = \boldsymbol{\omega}_1 \times \mathbf{R}_i. \tag{14}$$

Now let us introduce the absolute angular velocities of the bodies in their own axes. The angular velocities of the main body in $Cx_1y_1z_1$ and the damper-body in $Cx_2y_2z_2$ are:

$$\boldsymbol{\omega}_1 = \begin{bmatrix} p_1 \\ q_1 \\ r_1 \end{bmatrix}; \qquad \boldsymbol{\omega}_2 = \begin{bmatrix} p_2 \\ q_2 \\ r_2 \end{bmatrix}. \tag{15}$$

The relative angular velocity of the movable unit in its coordinates frame is:

$$\boldsymbol{\omega}_{r3} = \begin{bmatrix} \dot{\alpha}, \, 0, \, 0 \end{bmatrix}^T. \tag{16}$$

Then the absolute angular velocity of the movable unit is:

$$\boldsymbol{\omega}_3 = \boldsymbol{\delta}_{31}^{\mathbf{T}} \boldsymbol{\omega}_1 + \boldsymbol{\omega}_{r3}. \tag{17}$$

The relative angular velocity of the rotor in its own connected coordinates frame is:

$$\boldsymbol{\omega}_{r4} = \begin{bmatrix} 0, \, 0, \, \dot{\gamma} \end{bmatrix}^T. \tag{18}$$

Then the absolute angular velocity of the movable unit is:

$$\boldsymbol{\omega}_4 = \boldsymbol{\delta}_{43}^{\mathbf{T}} \boldsymbol{\omega}_3 + \boldsymbol{\omega}_{r4}. \tag{19}$$

The torques of viscous friction depend on the relative motion and can be written as follows:

$$\begin{aligned} \mathbf{M}_b &= -\nu \left(\boldsymbol{\omega}_1 - \boldsymbol{\Theta} \cdot \mathbf{B}^{-1} \cdot \boldsymbol{\omega}_2 \right); \\ \mathbf{M}_d &= -\nu \left(\boldsymbol{\omega}_2 - \mathbf{B} \cdot \boldsymbol{\Theta}^{-1} \cdot \boldsymbol{\omega}_1 \right); \end{aligned} \tag{20}$$

where ν - is the coefficient of the viscose friction, $\boldsymbol{\Theta}$ - is the transition matrix from the orbital coordinate frame CXYZ to the $C_1x_1y_1z_1$ coordinate system, $\mathbf{B}$ - is the transition matrix from the orbital coordinate frame to the $C_2x_2y_2z_2$ coordinate system.

To describe the attitude of bodies (the main body and the damper-body), we will use the "directional cosines" of the unit vectors $\{\mathbf{e}_\tau, \mathbf{e}_n, \mathbf{e}_r\}$ of axes of the orbital coordinates system CXYZ (fig.3) in corresponded connected coordinates systems of bodies ($C_1x_1y_1z_1$ and $C_2x_2y_2z_2$). Then the components of the unit vectors in the connected systems $C_1x_1y_1z_1$ and $C_2x_2y_2z_2$ have the form:

$$\begin{aligned} \mathbf{e}_{\tau i} &= \begin{bmatrix} \alpha_{i1}, \alpha_{i2}, \alpha_{i3} \end{bmatrix}^T; \\ \mathbf{e}_{ni} &= \begin{bmatrix} \beta_{i1}, \beta_{i2}, \beta_{i3} \end{bmatrix}^T; \\ \mathbf{e}_{ri} &= \begin{bmatrix} \gamma_{i1}, \gamma_{i2}, \gamma_{i3} \end{bmatrix}^T; \end{aligned} \tag{21}$$

where the index i=1, 2 indicates the bodies numbers.

The matrixes $\mathbf{\Theta}$ and $\mathbf{B}$ -in terms of directional cosines will have the following structure:

$$\mathbf{\Theta} = \begin{bmatrix} \alpha_{11} & \beta_{11} & \gamma_{11} \\ \alpha_{12} & \beta_{12} & \gamma_{12} \\ \alpha_{13} & \beta_{13} & \gamma_{13} \end{bmatrix}, \quad \mathbf{B} = \begin{bmatrix} \alpha_{21} & \beta_{21} & \gamma_{21} \\ \alpha_{22} & \beta_{22} & \gamma_{22} \\ \alpha_{23} & \beta_{23} & \gamma_{23} \end{bmatrix}. \tag{22}$$

The gravitational torques acting on the on the damper-body can be written in their own connected frames as follows:

$$\mathbf{M}_{gd} = 3\omega_0^2 \left(\mathbf{e}_{r2} \times \mathbf{I}_2 \mathbf{e}_{r2} \right) = 3\omega_0^2 \left(\left(\mathbf{B} \cdot [0,0,1]^T \right) \times \mathbf{I}_2 \left(\mathbf{B} \cdot [0,0,1]^T \right) \right). \tag{23}$$

The gravitational torque acting on the subsystem (excluding the damper) around the common center of mass can be calculated as the sum of the corresponding parts. Here it is needed to take into account the terms from the difference of components of central tensors of inertia of bodies calculated in their own frames of coordinates, and, additionally, from a gravitational dumbbell, formed by the distant between centers of mass of the main body (C_1) and the movable unit with the rotor ($C_3 \equiv C_4$):

$$\mathbf{M}_{gb} = 3\omega_0^2 \left[\left(\mathbf{e}_{r1} \times \mathbf{I}_1 \mathbf{e}_{r1} \right) + \delta_{31} \left(\left(\delta_{13} \mathbf{e}_{r1} \right) \times \mathbf{I}_3 \left(\delta_{13} \mathbf{e}_{r1} \right) \right) + \delta_{41} \left(\left(\delta_{14} \mathbf{e}_{r1} \right) \times \mathbf{I}_4 \left(\delta_{14} \mathbf{e}_{r1} \right) \right) + \left(\mathbf{e}_{r1} \times \mathbf{J} \mathbf{e}_{r1} \right) \right], \tag{24}$$

where

$$\mathbf{J} = \mathrm{diag} \left[m_1 |\mathbf{R}_1|^2 + (m_3 + m_4) |\mathbf{R}_3|^2 ; \quad m_1 |\mathbf{R}_1|^2 + (m_3 + m_4) |\mathbf{R}_3|^2 ; \quad 0 \right]. \tag{25}$$

The tensor $\mathbf{J}$ represents the inertia tensor of the indicated gravitational dumbbell; and the scalar value ω_0 is the angular velocity of the orbital coordinate system (the angular velocity of the orbital motion around the Earth along circle orbit).

Now we should add the kinematical expressions taking into account the orbital rotation. We will use the well-known expressions to the unit vectors of the orbital system [e.g., 11]:

$$\begin{cases} \dfrac{d\mathbf{e}_{ri}}{dt} = \mathbf{e}_{ri} \times \boldsymbol{\omega}_i + \omega_0 \mathbf{e}_{\tau i}; \\[2mm] \dfrac{d\mathbf{e}_{ni}}{dt} = \mathbf{e}_{ni} \times \boldsymbol{\omega}_i; \\[2mm] \dfrac{d\mathbf{e}_{\tau i}}{dt} = \mathbf{e}_{\tau i} \times \boldsymbol{\omega}_i - \omega_0 \mathbf{e}_{ri}; \end{cases} \tag{26}$$

where $i=1, 2$.

So, the equations (1), (26) completely describe the angular motion of our mechanical system at the consideration of angles and angular velocities $\{\alpha, \dot{\alpha}, \gamma, \dot{\gamma}\}$ as controlling parameters described by control laws. In our research, we synthesized the following control laws:

$$\dot{\alpha} = k_p p_1 - k_\alpha \alpha; \tag{27}$$

$$\dot{\gamma} = \Omega \mathrm{H} \left(r_1 \alpha \right); \tag{28}$$

where k_p, k_α are the feedback gain constants, Ω – is the predefined constant of the value of the angular velocity of the rotor, and H(·) – is the Heaviside function:

$$H\left(\xi\right)=\begin{cases}1, & \xi>0 \\ 0, & \xi\leq 0\end{cases} \tag{29}$$

The logic of the control laws (27) and (28) is based on the natural properties of the dynamics. To explain this, we can remind the conservation of angular momentum law: the complete angular momentum of the closed torque-free mechanical system remains constant, but the system elements can exchange angular momentum parts between themselves. Therefore, in our idea, to minimize the transversal angular velocity p of the main body, we should to increase the angular velocity $\dot\alpha$ of the movable unit (proportionally to current value of the velocity p), then the main body translates the corresponded angular momentum to the movable unit (27). The law (28) uses the pulse activation of the rotor constant angular velocity to create the gyroscopic torque to combine the axes of the main body and the movable unit. As it follows from the form of the law (28), the rotor will turn on when the longitudinal angular velocity r_1 and the angle α are simultaneously nonzero. At the action of the external gravitational torques and internal dissipation, the indicated natural tendencies of the angular momentum exchange between the system bodies will minimize the angular velocities of all bodies.

To show the stability of the considered controlled motion it is possible to use the approach with the Lyapunov function. For these purposes, let us introduce the relative (with respect to the orbital coordinates frame) angular velocities of bodies (i=1, 2):

$$\tilde{\boldsymbol{\omega}}_i = \boldsymbol{\omega}_i - \omega_0 \mathbf{e}_{ni}. \tag{30}$$

To build the Lyapunov functions we can use the Beletsky integral [11]:

$$V=\frac{1}{2}\Big[\tilde{\boldsymbol{\omega}}_1 \mathbf{I}_s \tilde{\boldsymbol{\omega}}_1 + 3\omega_0^2 \mathbf{e}_{r1}\mathbf{I}_s\mathbf{e}_{r1} - \omega_0^2 \mathbf{e}_{n1}\mathbf{I}_s\mathbf{e}_{n1} + \tilde{\boldsymbol{\omega}}_2 \mathbf{I}_2 \tilde{\boldsymbol{\omega}}_2 + 3\omega_0^2 \mathbf{e}_{r2}\mathbf{I}_2\mathbf{e}_{r2} - \omega_0^2 \mathbf{e}_{n2}\mathbf{I}_2\mathbf{e}_{n2}\Big] \tag{31}$$

where $\mathbf{I}_s = \mathbf{I}_1 + \mathbf{I}_3 + \mathbf{I}_4 + \mathbf{J}$ – is the summarized inertia tensor of the satellite with the immovable unit and the rotor $\left(\alpha \equiv \gamma \equiv 0\right)$. The form (31) describes the motion "first integral" of a conservative mechanical system with two rigid bodies without the internal interaction: the first rigid body is formed by the subsystem of the main body (#1), the unit (#3), the rotor (#4) without any relative motions of these elements, and the second rigid body is the damper-body (#2). So, without the internal friction we will have the conservative case, and the complete energy of the system in the central gravitational field (31) will be preserved. However, the internal friction between the main body and the damper-body will decrease the complete energy due to dissipation properties, but we still can use the form (31) in the role of the Lyapunov function as the natural energy expression. As

can we see from (31), the function V is the scalar function depended on the set of variables $\left\{ \tilde{p}_i, \tilde{q}_i, \tilde{r}_i, \beta_{ij}, \gamma_{ij} \right\}_{i=(1,2), j=(1,2,3)}$. The following geometrical expressions are obvious:

$$\begin{cases} \gamma_{i3}^2 = 1 - \gamma_{i1}^2 - \gamma_{i2}^2; \\ \beta_{i2}^2 = 1 - \beta_{i1}^2 - \beta_{i3}^2. \end{cases} \tag{32}$$

The substitution of expressions (32) in the function (31) allows to exclude from the consideration the variables $\left\{ \gamma_{i3}, \beta_{i2} \right\}$, and then we will have the function V depended from fourteen variables:

$$V = V\left(\tilde{p}_1, \tilde{q}_1, \tilde{r}_1, \tilde{p}_2, \tilde{q}_2, \tilde{r}_2, \beta_{11}, \beta_{13}, \beta_{21}, \beta_{23}, \gamma_{11}, \gamma_{12}, \gamma_{21}, \gamma_{22} \right). \tag{33}$$

Taking into account the diagonal form of tensors $\mathbf{I}_s$, $\mathbf{I}_1$, $\mathbf{I}_3$, $\mathbf{I}_4$, $\mathbf{J}$, it is possible to conclude that the function (33) represents the quadratic form. For example, the partial dependencies of terms of L, from the corresponded variables are depicted at the fig.4. From the fig.4 we see the surfaces of growing paraboloids. By subtracting the constant $V(\mathbf{0})$ we obtain the positive-definite quadratic form, which can be used in the role of the classical Lyapunov function:

$$L\left(\tilde{p}_1, \tilde{q}_1, \tilde{r}_1, \tilde{p}_2, \tilde{q}_2, \tilde{r}_2, \beta_{11}, \beta_{13}, \beta_{21}, \beta_{23}, \gamma_{11}, \gamma_{12}, \gamma_{21}, \gamma_{22} \right) = V - V(\mathbf{0}). \tag{34}$$

Moreover, in the gravitational equilibrium position the variables $\left\{ \tilde{p}_1, \tilde{q}_1, \tilde{r}_1, \tilde{p}_2, \tilde{q}_2, \tilde{r}_2, \beta_{11}, \beta_{13}, \beta_{21}, \beta_{23}, \gamma_{11}, \gamma_{12}, \gamma_{21}, \gamma_{22} \right\}$ are equal to zero values, and, therefore, all of them also can be considered as small deviations in the classical Lyapunov stability theory.

The pure analytical investigation of the Lyapunov function (34) derivative is quite problematic, but we can use the numerical modeling by numerical integrating the motion equations. In the presence of the internal friction with the damper and also at the action of control torques (27) and (28), the conservativeness of the system will be destroyed and the Beletsky integral will not save its constant value. Nevertheless, we can still use the Lyapunov function in the form (34) to study the stability of the motion mode that brings the nanosatellite to the gravitational equilibrium position. The numerical modeling results are presented at the fig.14.
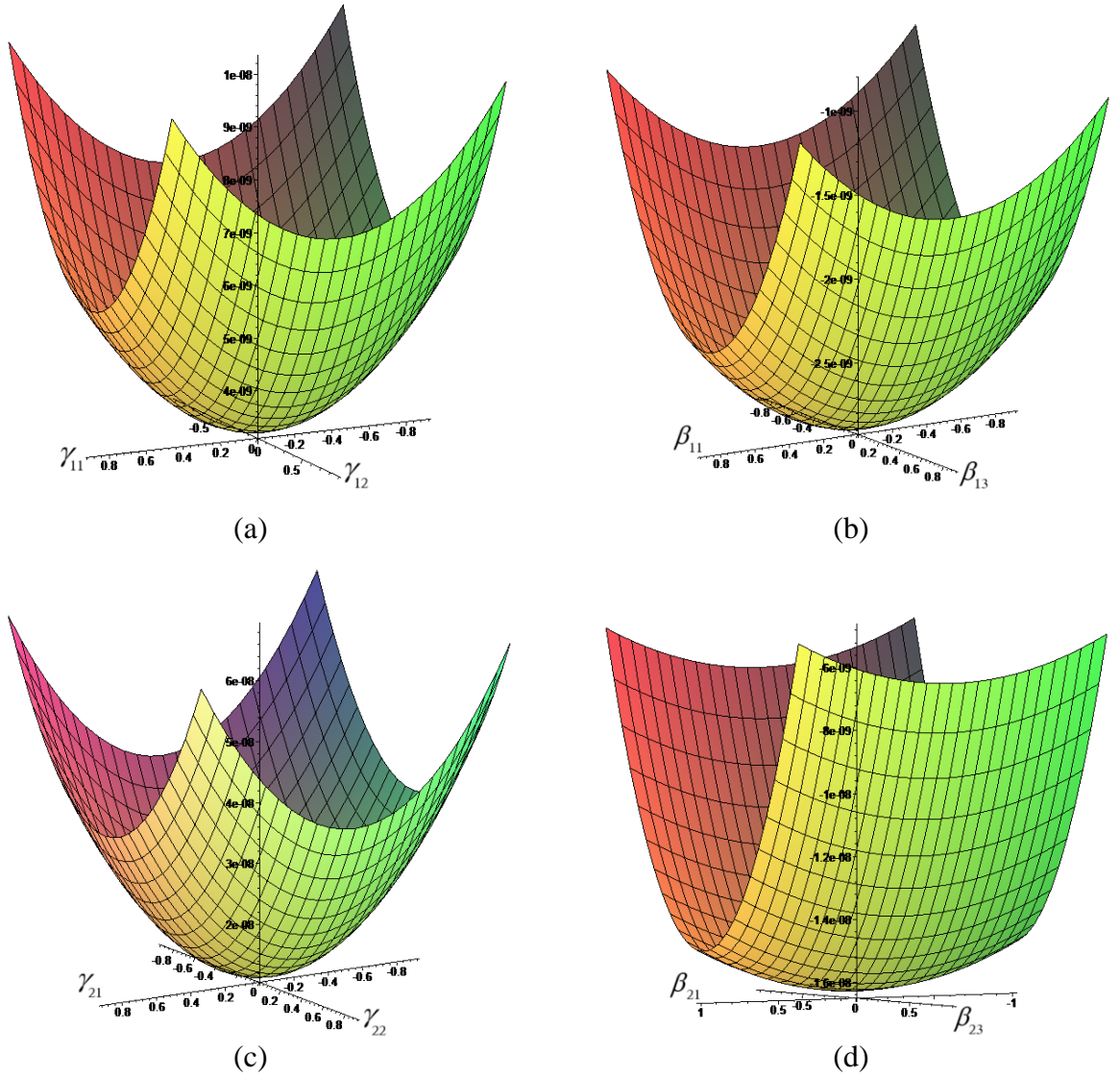
(a)

(b)

(c)

(d)

Figure 4 – Parabolic surfaces of terms of the function (33):

(a) the term $\dfrac{3}{2}\omega_0^2 \mathbf{e}_{r1}\mathbf{I}_s\mathbf{e}_{r1}$;   (b) the term $\dfrac{1}{2}\left(-\omega_0^2 \mathbf{e}_{n1}\mathbf{I}_s\mathbf{e}_{n1}\right)$;

(c) the term $\dfrac{3}{2}\omega_0^2 \mathbf{e}_{r2}\mathbf{I}_2\mathbf{e}_{r2}$;   (d) the term $\dfrac{1}{2}\left(-\omega_0^2 \mathbf{e}_{n2}\mathbf{I}_2\mathbf{e}_{n2}\right)$.

At the fig.14 two cases of motion are presented: the first case – is the motion of the nanosatellite with the movability of the internal damper, but at the fixation of the unit and the rotor (we can call this as the "rigid bodies" case); the second case corresponds to the controlled motion of the system. As can we see from the obtained results (fig.14), the both cases are characterized by the decreasing Lyapunov function with the negative derivative, and, therefore, the both regimes are stable. However, the case with the control has a significantly stronger and faster exponential convergence to zero in comparison with the "rigid bodies" case – this confirms the effectiveness of the synthesized control laws (27) and (28).

In the practical sense we can note, that to implement the control laws (27) and (28), we need to know the current values of the angular velocity of the main body and the angle of the movable unit deflection. To find out these parameters on board of the nanosatellite, it is possible to use the angular velocity sensors, and the α-angle sensor (or the integrator the of $\alpha(t)$ value from (27)). All indicated sensors can be chosen from the broad spectrum of simple small microelectromechanical systems, e.g. MEMS gyroscopes and linear/angular sensors [40-42].

Now on the base of equations (1), (26) and laws (27), (28) we have the complete mathematical model to simulate the system attitude dynamics. As it is known, to the numerical simulation realization we need to integrate numerically the differential equations with the help of standard numerical methods (the Runge–Kutta family of methods, the Rosenbrock method, etc.), which use the standard form of the equations with the right-hand sides resolved with respect to higher derivatives. In this connection, we also built this standard form of the differential equations. In our case, the corresponding standard form of these equations is cumbersome, and it does not presented here in the paper. The analytical standard form of the equations was automatically built in the mathematical package "Maple". This standard form has no scientific value and it is only used for numerical calculations by the Rosenbrock integration method in the "Maple" software.

The corresponded numerical simulation results are presented in the next section of the paper. To this simulation, we used initial conditions and inertia-mass parameters from tables 1 and 2.

4. RESULTS

To show the workability of the constructed damping scheme, arising the final gravitational equilibrium position, and the effectiveness of the synthesized control laws we will provide the numerical investigation of two cases of the nanosatellite attitude dynamics on the base of equations (1), (26) and laws (27), (28).

The first case corresponds to the fixed movable unit with the immovable rotor – this was above called as the "rigid bodies" case. Simulation results for the first case are presented at figures 5-12 with liter (a).

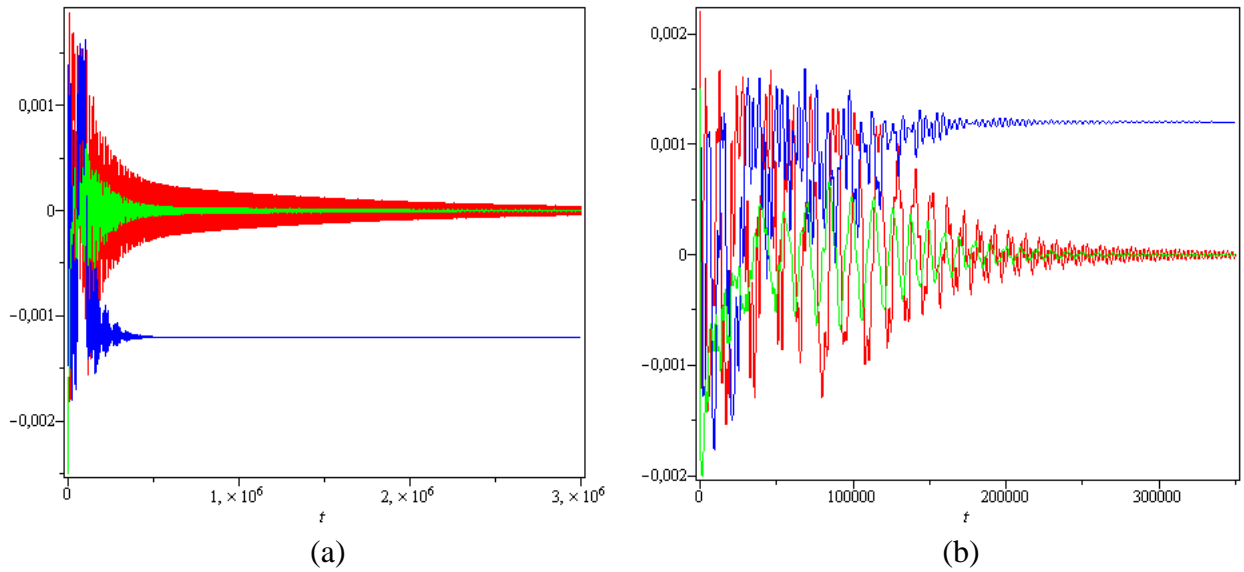(a)   (b)

Figure 5 – Time-evolutions of the angular velocity components $p_1(t)$ (in red), $q_1(t)$ (in blue),

$r_1(t)$ (in green) of the main body:

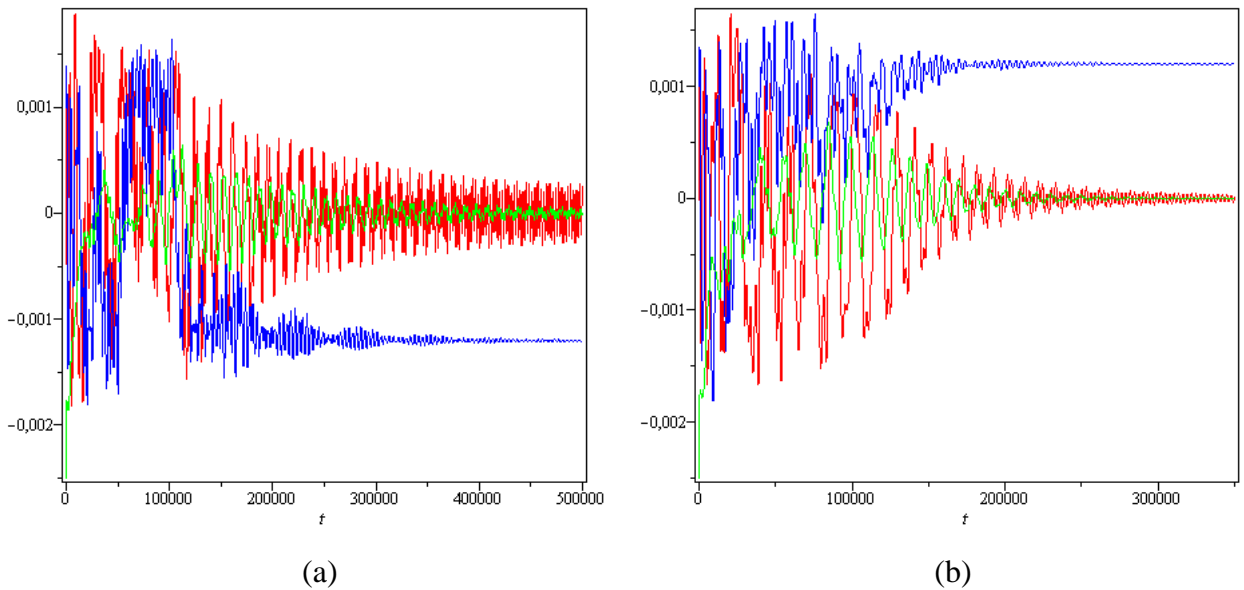(a) – the "rigid bodies" case; (b) – the case with the control (27) and (28)

(a)   (b)

Figure 6 – Time-evolutions of the angular velocity components $p_2(t)$ (in red), $q_2(t)$ (in blue),

$r_2(t)$ (in green) of the damper:

(a) – the "rigid bodies" case; (b) – the case with the control (27) and (28)
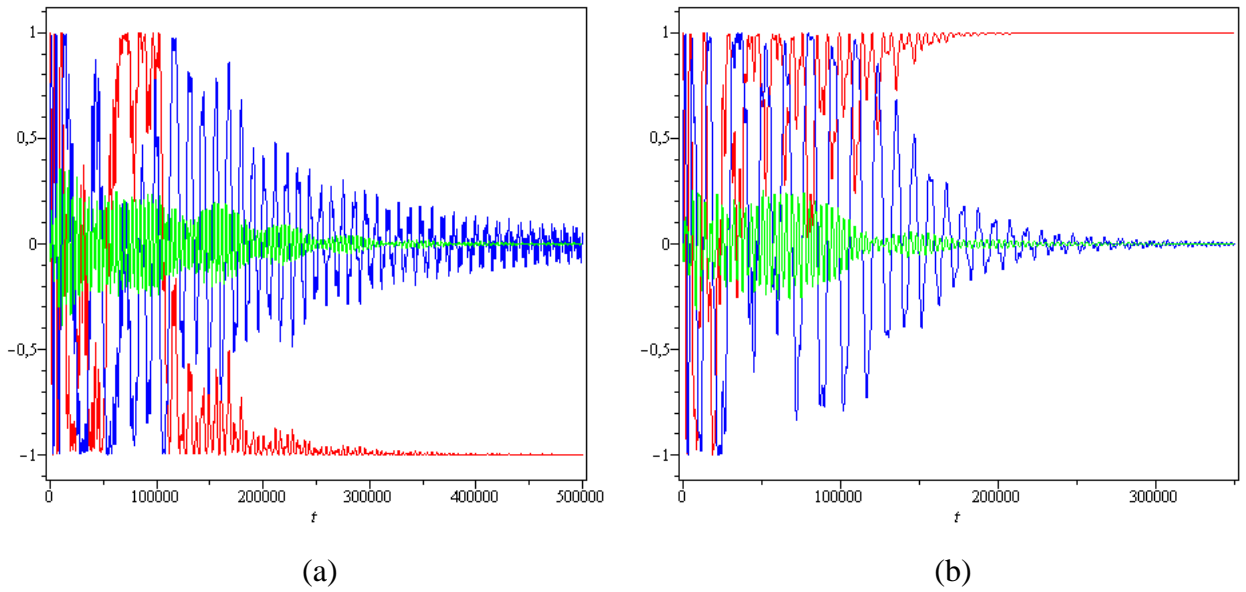
16

(a)   (b)

Figure 7 – The time-evolution of the directional cosines $\alpha_{11}(t)$ (red), $\alpha_{12}(t)$ (blue), $\alpha_{13}(t)$ (green) of the main body:
(a) – the "rigid bodies" case; (b) – the case with the control (27) and (28)
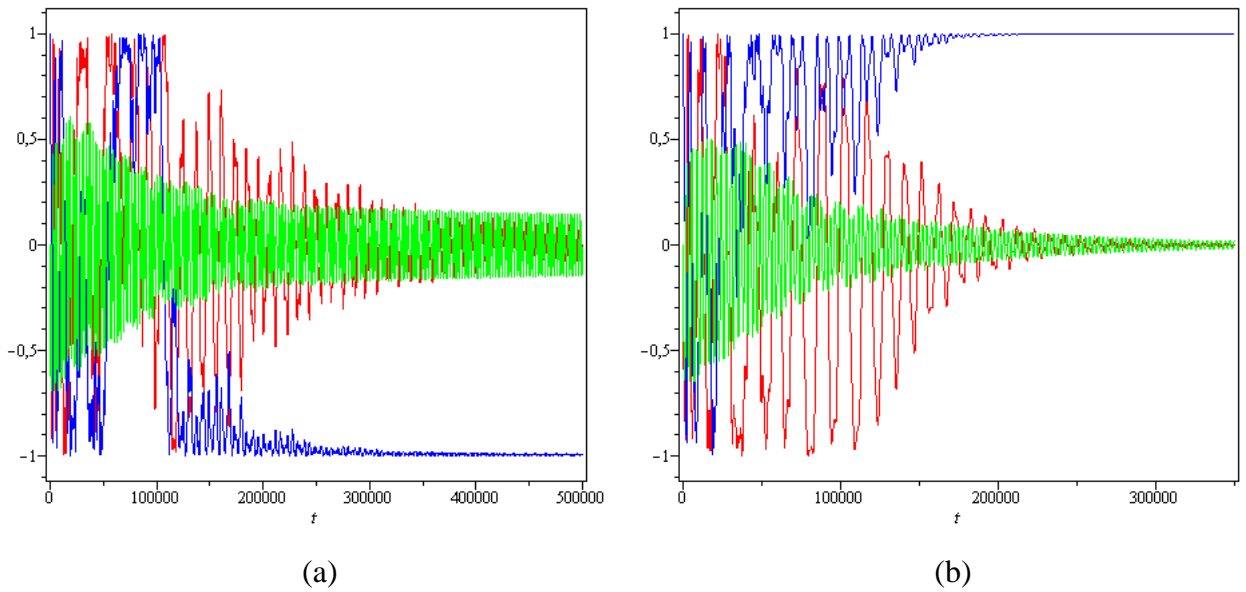

(a)   (b)

Figure 8 – The time-evolution of the directional cosines $\beta_{11}(t)$ (red), $\beta_{12}(t)$ (blue), $\beta_{13}(t)$ (green) of the main body:
(a) – the "rigid bodies" case; (b) – the case with the control (27) and (28)
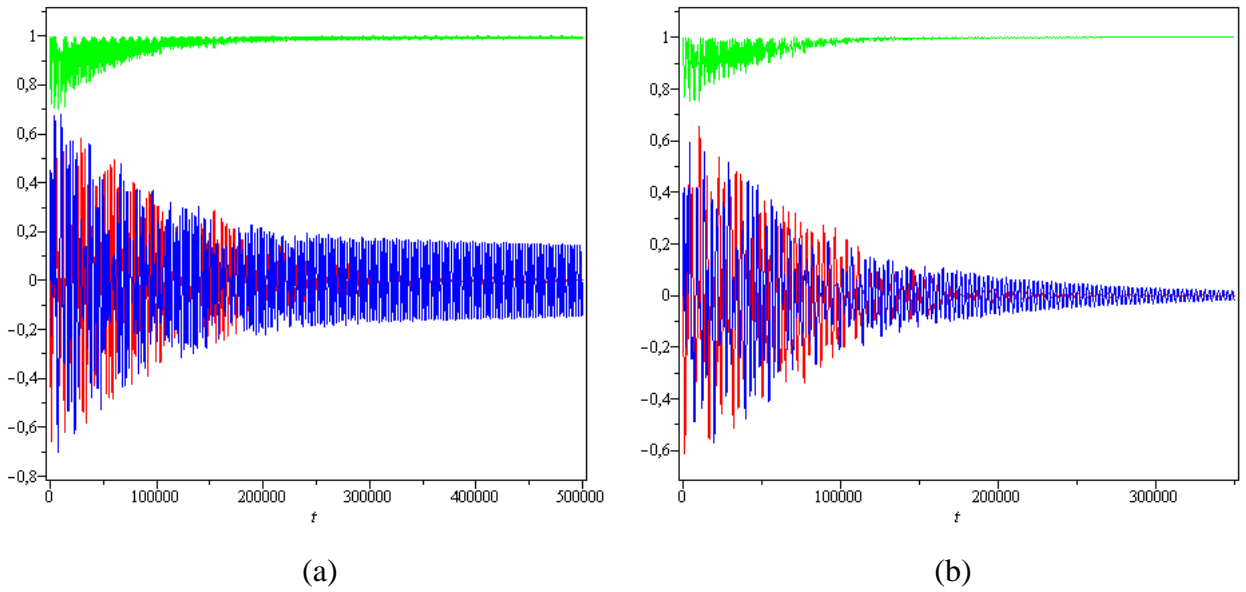
(a)   (b)

Figure 9 – The time-evolution of the directional cosines $\gamma_{11}(t)$ (red), $\gamma_{12}(t)$ (blue), $\gamma_{13}(t)$ (green) of the main body:
(a) – the "rigid bodies" case; (b) – the case with the control (27) and (28)
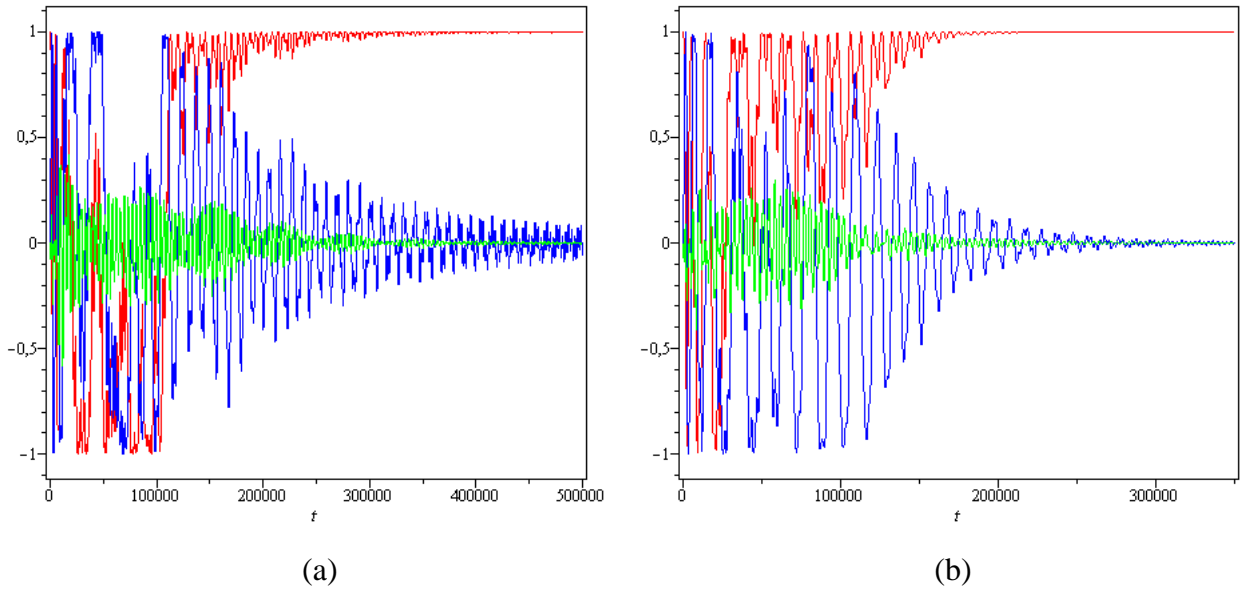

(a)   (b)

Figure 10 – The time-evolution of the directional cosines $\alpha_{21}(t)$ (red), $\alpha_{22}(t)$ (blue), $\alpha_{23}(t)$ (green) of the damper body:
(a) – the "rigid bodies" case; (b) – the case with the control (27) and (28)

18

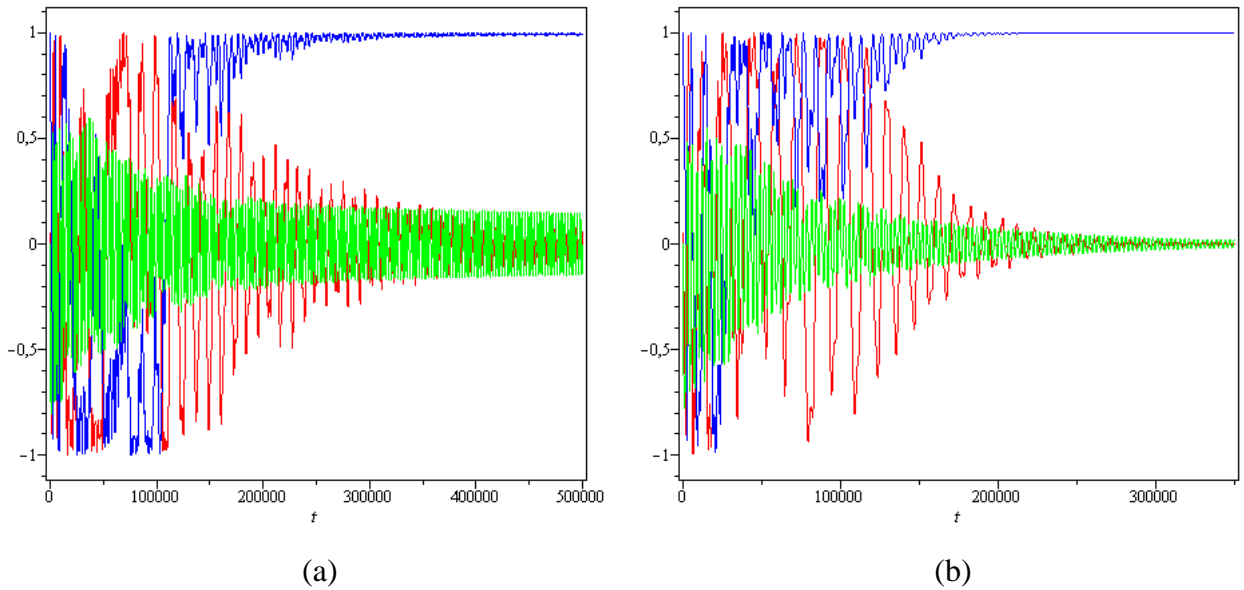(a)   (b)

Figure 11 – The time-evolution of the directional cosines $\beta_{21}(t)$ (red), $\beta_{22}(t)$ (blue), $\beta_{23}(t)$ (green) of the damper body:
(a) – the "rigid bodies" case; (b) – the case with the control (27) and (28)

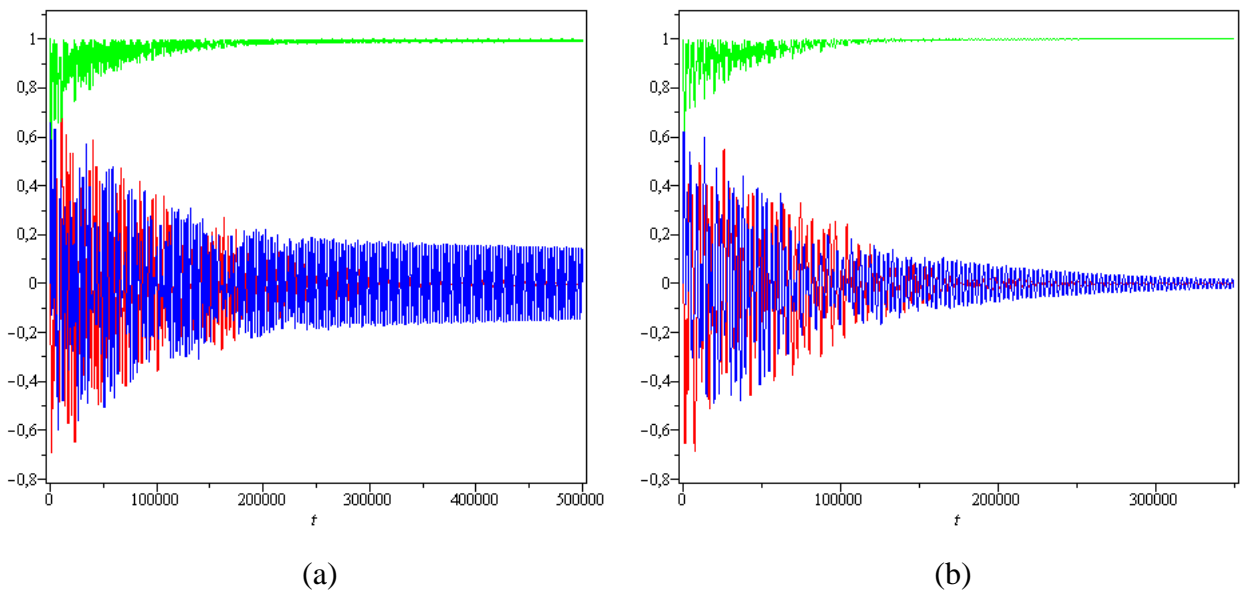(a)   (b)

Figure 12 – The time-evolution of the directional cosines $\gamma_{21}(t)$ (red), $\gamma_{22}(t)$ (blue), $\gamma_{23}(t)$ (green) of the damper body:
(a) – the "rigid bodies" case; (b) – the case with the control (27) and (28)

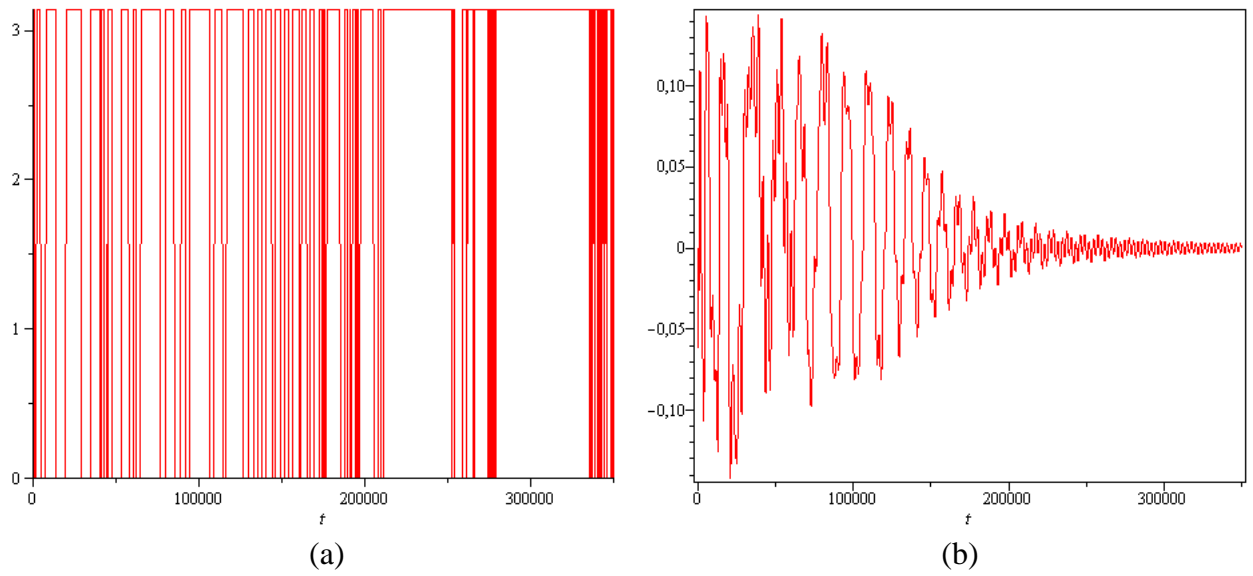(a)   (b)

Figure 13 – The time-evolution in the case with the control (27) and (28):
(a) – the rotor angular velocity $\dot{\gamma}(t)$; (b) – the deflection angle of the movable unit $\alpha(t)$
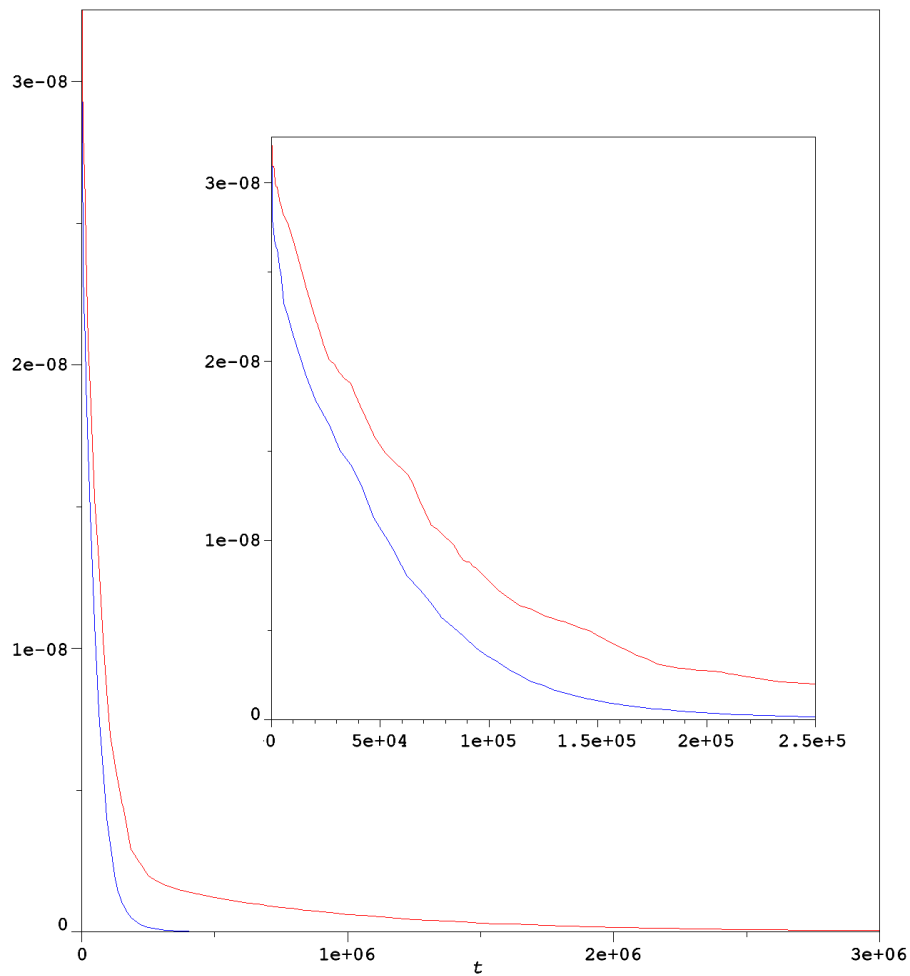

Figure 14 – The Lyapunov function time-evolution in the "rigid bodies" case (red) and in the case with the control (27) and (28) (blue)

First of all, as can we see from fig.5-a and fig.14, the "rigid bodies" scheme achieved the stable gravitational equilibrium after $3 \cdot 10^6$ seconds, when residual values of the components p_1 and r_1 of the angular velocity of the main body will become equal to $\sim 10^{-4}$ rad/s, when the component q_1 will reach the orbital angular velocity value $\left(q_1 = \pm \omega_0 \right)$ and when the direction cosines will confirm the coincidence of the axes of the connected and the orbital coordinates frames. In addition, the gravitational equilibrium obtainment can be indicated by the Lyapunov function values, which will be close to zero (fig.14, red line) due to zeroing out small deviations. At the fig.6-a – fig.13-a the plotting time interval is decreased to show details of motion phases with active dynamics.

So, we can conclude that in this case of the modeling, the stable final attitude position of the nanosatellite will be obtained after $3 \cdot 10^6$ seconds.

The second case describes the motion of the nanosatellite with the movability of the unit and the rotor with control laws (27) and (28). Simulation results are shown in figures 5-13 with liter (b). The time-history of the movable unit motion and the piecewise continuous rotation of the rotor presented at fig.13. All numerical results demonstrate the steady process of the gradual transition to the gravitational stable position of the nanosatellite on the orbit.

In this case, as we can see from the numerical modelling, the gravitational stabilization is obtained after $3 \cdot 10^5$ seconds. This allows to confirm, that the controlled stabilization is fulfilling most quickly in comparison with the uncontrolled case of "rigid bodies".

We see practically tenfold increase in speed of the stabilization process ($3 \cdot 10^5$ vs $3 \cdot 10^6$ seconds) – this is the evident confirmation of the effectiveness of the synthesized control laws (27) and (28).

1

2   TABLE 1. INITIAL CONDITIONS

Parameter	Unit	Value
p_1	rad/s	0.0015
q_1	rad/s	0.002
r_1	rad/s	-0.004
p_2	rad/s	0.002
q_2	rad/s	0.001
r_2	rad/s	0.0015
$\theta_1 = \beta_1$	rad	0.015
$\theta_2 = \beta_2$	rad	0.01
$\theta_3 = \beta_3$	rad	0.02
$\dot{\gamma}$	rad/s	0
α	rad	0
ω_0	rad/s	0.0012

3

4   TABLE 2. INERTIAL-MASS PARAMETERS

Parameter	Unit	Value
A_1	$kg \cdot m^2$	0.0045
B_1	$kg \cdot m^2$	0.0055
C_1	$kg \cdot m^2$	0.0035
A_2	$kg \cdot m^2$	0.003
B_2	$kg \cdot m^2$	0.004
C_2	$kg \cdot m^2$	0.0015
A_3	$kg \cdot m^2$	0.0025
B_3	$kg \cdot m^2$	0.0035
C_3	$kg \cdot m^2$	0.0015
$A_4 = B_4$	$kg \cdot m^2$	0.0002
C_4	$kg \cdot m^2$	0.0004
m_1	kg	2
m_2	kg	0.5
m_3	kg	1
m_4	kg	0.04
l_1	m	0.1
l_3	m	0.04
l_4	m	0.04
k_α	s^{-1}	0.008
k_p	[1]	-0.7
Ω	s^{-1}	3.14
ν	$N \cdot m \cdot s$	0.00001

5

As we can see, the main goal of the research is reached. In the controlled motion with laws (27) and (28) the nanosatellite proceeds into the gravitational stabilization position more effective in comparison with the uncontrolled passive case (about ten times). Nonetheless, here it is worth to discuss some aspects of the satellites stabilization tasks, and some other connected questions.

First of all, we should note, that some alternative schemes of the spatial position stabilizations can be used in the practice of the space missions; and different types of the dampers can be selected to achieve the predefined attitude. In simplest cases, it is possible to consider the attitude dynamics of the satellites as the torque-free dynamics, and then the simplest form of the damper will quite useful. For example, it is possible to indicate the simple spherical cavities filled with liquids (a liquid fuel). Then these cavities will play role of the dampers due to creation of the internal friction, which can smoothly stop the attitude motion or undesirable forms of angular motion (e.g., a parasitic nutation) [12]. Also in such cases, the simple oscillatory systems with viscous friction are applied [13, 14]. The oscillating masses with damping in spacecraft with partially filled cavities with liquid also are one of type of effective dampers [15, 16]. In some missions, it will be enough to achieve the spatial orientation along the forces lines of the geomagnetic field, and then the magnetic dampers are quite appropriate in theirs different constructional forms and at a diversity of the control laws [17-22]. Moreover, the magnetic dampers also used in the spacecraft missions with gravity gradient stabilization [23, 24]. Some alternative schemes of damping are possible, including the fluid rings or pendulum dampers [25-27]. It is worth to indicate the other control methods, which can be used to the attitude motion control under the presence of perturbations [27-30]. In addition, we should underline effective approaches of spacecraft stabilization and control, based on active schemes of gravity-gradient stabilization [31, 32], on integrated magnetic and impulsive actuators [33-37], on schemes specialized in concrete modes [38] or adapted to new platforms of satellites [39].

All indicated above schemes of attitude stabilization are useful and each of them can be most appropriate to solve the practical tasks of a concrete space mission. With directly regard to gravitational dampers, it can be noted that the classical variant of the damper represents the spherically symmetrical rigid body with the corresponding spherical inertia tensor – this classical type [1-5], as well as the simple cavities filled with viscous liquids [12], will fulfill the process of damping the attitude oscillations around the stable spatial position. In the considered research the generalized scheme of the gravitational damper was considered, when the damper-body has three-axial inertia tensor. The using damper-body with the three-axial inertia tensor significantly

complicates the mathematical model and requires taking into account the relative position of both bodies (the main body and the damper-body) with respect to the gravity gradient vector. However, in this generalized scheme, it is obvious that we will have a gain in the efficiency of the damping process.

Thus, we invite readers and researchers to get involved in the research of the attitude dynamics and control of the nanosatellites with the movable elements, and into synthesis and comparing models and efficiency of the classical and the generalized schemes of the gravitational damper.

Conclusion

As we can see, the main goal of the research was reached. In the controlled motion with the synthesized control laws the nanosatellite proceeds into the gravitational stabilization position more effective in comparison with the uncontrolled passive case. The main feature here is the use of the controlled movability of the constructional elements of the nanosatellite. When we allow the relative motion of the movable parts, then the dynamics goes into more complex but more effective process, where the gravity and the gyroscopic torque from the controlled deflecting rotor will help each other - this allows us to develop new control laws for the attitude dynamics and attitude positioning of nanosatellites of similar constructions. The ten times increasing in the efficiency of the stabilizing process take place at the control of movable parts of the nanosatellite.

References

[1]   Chernous'ko, F. L. (1968). Motion of a solidcontaininga spherical damper. Journal of Applied Mechanics and Technical Physics, 9(1), 45-48.

[2]   F. L. Chernous'ko, Motion of a Solid Body with Cavities Filled with a Viscous Fluid. VTs AN SSSR, Moscow (1968).

[3]   Amelkin, N. I., & Kholoshchak, V. V. (2017). Stability of the steady rotations of a satellite with internal damping in a central gravitational field. Journal of Applied Mathematics and Mechanics, 81(2), 85-94.

[4]   Amel'kin, N. I., & Kholoshchak, V. V. (2019). Rotational motion of a non-symmetrical satellite with a damper in a circular orbit. Mechanics of Solids, 54(2), 190-203.

[5]   Amel'kin, N. I. (2020). Evolution of Rotational Motion of a Planet in a Circular Orbit Under the Influence of Internal Elastic and Dissipative Forces. Mechanics of Solids, 55(2),

234-247.

[6]   L. K. Davis, "Motion damper" U.S. Patent No. 3,399,317. Washington, DC: U.S. Patent and Trademark Office (1968).

[7]   Applied celestial mechanics and motion control. Collection of articles dedicated to the 90th anniversary of the birth of D.E. Okhotsimsky / Compiled by: T.M. Eneev, M.Yu. Ovchinnikov, A.R. Golikov. - Moscow: IPM im. M.V. Keldysh, 2010. - 368 p. — ISBN 978-5-98354-007-1.

[8]   Doroshin, A. V. (2022). Gravitational Dampers for Unloading Angular Momentum of Nanosatellites. In: Lacarbonara, W., Balachandran, B., Leamy, M.J., Ma, J., Tenreiro Machado, J.A., Stepan, G. (eds) Advances in Nonlinear Dynamics. NODYCON Conference Proceedings Series. Springer, Cham. https://doi.org/10.1007/978-3-030-81162-4_23.

[9]   Doroshin A. V. Nutational oscillations suppression in attitude dynamics of spacecraft by relative motion of its movable module/ A. V. Doroshin, A. V Eremenko// J. Phys.: Conf. Ser – 2019.

[10]   Doroshin, A. V. Attitude control of nanosatellite with single thruster using relative displacements of movable unit / A. V. Doroshin, A. V. Eremenko// Proceedings of the Institution of Mechanical Engineers, Part G: Journal of Aerospace Engineering. – 2021, pp.758-767.

[11]   Beletsky V. V. Satellite Motion Relative to the Center of Mass in a Gravitational Field (Dvizhenie Sputnika Otnositel'no Tsentra Mass v Gravitatsionnom Pole), Moscow: Mosk. Gos. Univ., 1975.

[12]   Winfree, P. K., & Cochran Jr, J. E. (1986). Nonlinear attitude motion of a dual-spin spacecraft containing spherical dampers. Journal of Guidance, Control, and Dynamics, 9(6), 681-690.

[13]   Sandfry, R., & Hall, C. (2000, August). Motion of a Gyrostat with a Discrete Damper. In Astrodynamics Specialist Conference (p. 4534).

[14]   Sandfry, R. A., & Hall, C. D. (2004). Steady spins and spinup dynamics of axisymmetric dual-spin satellites with dampers. Journal of spacecraft and rockets, 41(6), 948-955.

[15]   Ayoubi, M. A., Goodarzi, F. A., & Banerjee, A. (2011). Attitude motion of a spinning spacecraft with fuel sloshing and nutation damping. The Journal of the Astronautical Sciences, 58(4), 551-568.

[16]   Mazmanyan, L., & Ayoubi, M. A. (2013, August). Attitude motion of a spinning spacecraft with fuel sloshing in high-G maneuvers. In Proc. AAS/AIAA Astrodyn. Spec. Conf. (pp. 793-812).

[17]   Ovchinnikov, M. Y., Pen'kov, V. I., Roldugin, D. S., & Karpenko, S. O. (2012). Investigation of the effectiveness of an algorithm of active magnetic damping. Cosmic Research, 50, 170-176.

[18]   Ovchinnikov, M. Y. (2012). Attitude dynamics of a small-sized satellite equipped

with hysteresis damper. Advances in the Astronautical Sciences, pp. 311-330.

[19]   Ovchinnikov, M. Y., Roldugin, D. S., & Penkov, V. I. (2012). Asymptotic study of a complete magnetic attitude control cycle providing a single-axis orientation. Acta Astronautica, 77, 48-60.

[20]   Ivanov, D. S., Ovchinnikov, M. Y., Penkov, V. I., & Ivanova, T. A. (2020). Modeling a nanosatellite's angular motion damping using a hysteresis plate. Mathematical Models and Computer Simulations, 12, 816-823.

[21]   Ovchinnikov, M. Y., & Roldugin, D. S. (2019). A survey on active magnetic attitude control algorithms for small satellites. Progress in Aerospace Sciences, 109, 100546.

[22]   Roldugin, D. S., & Ovchinnikov, M. Y. (2023). Wobble of a spin stabilized satellite with cross products of inertia and magnetic attitude control. Advances in Space Research, 71(1), 408-419.

[23]   Arduini, C., & Baiocco, P. (1997). Active magnetic damping attitude control for gravity gradient stabilized spacecraft. Journal of Guidance, Control, and Dynamics, 20(1), 117-122.

[24]   Gama, R., Guerman, A. D., Seabra, A., & Smirnov, G. V. (2013). Averaging methods for design of spacecraft hysteresis damper. Mathematical Problems in Engineering, 2013

[25]   Kumar, K. D. (2009). Satellite attitude stabilization using fluid rings. Acta Mechanica, 208(1-2), 117-131.

[26]   Nobari, N. A., & Misra, A. K. (2012). Attitude dynamics and control of satellites with fluid ring actuators. Journal of Guidance, Control, and Dynamics, 35(6), 1855-1864.

[27]   Filimonikhin, G. B., Pirogov, V. V., & Filimonikhina, I. I. (2007). Attitude stabilization of the rotational axis of a carrying body by pendulum dampers. International Applied Mechanics, 43, 1167-1173.

[28]   Shiyou, Y., Ali, A., Rao, S., Fahad, S., Jing, W., Tong, J., & Tahir, M. (2022). Active attitude control for microspacecraft; A survey and new embedded designs. Advances in Space Research, 69(10), 3741-3769.

[29]   Yao, Q. (2021). Robust finite-time control design for attitude stabilization of spacecraft under measurement uncertainties. Advances in Space Research, 68(8), 3159-3175.

[30]   Cilden-Guler, D., Kaymaz, Z., & Hajiyev, C. (2023). Geomagnetic storms in the context of spacecraft attitude estimation under different noise levels. Advances in Space Research, 72(7), 2733-2740.

[31]   Ashenberg, Joshua, and Enrico C. Lorenzini. (1999). Active gravity-gradient stabilization of a satellite in elliptic orbits. Acta Astronautica 45 (10), 619-627.

[32]   Martel, Francois, Parimal Pal, and Mark Psiaki. Active magnetic control system for gravity gradient stabilized spacecraft, 1988.

[33]   Colagrossi, A. (2023). Integrated Magnetic Management of Stored Angular Momentum in Autonomous Attitude Control Systems. Aerospace, 10(2), 103.

[34]   Sharifi, E., & Damaren, C. J. (2020). Nonlinear optimal approach to spacecraft attitude control using magnetic and impulsive actuations. Journal of Guidance, Control, and Dynamics, 43(6), 1154-1163.

[35]   Damaren, C. J. (2002). Comments on "Fully magnetic attitude control for spacecraft subject to gravity gradient". Automatica, 38(12), 2189.

[36]   Colagrossi, A., & Lavagna, M. (2018). Fully magnetic attitude control subsystem for picosat platforms. Advances in Space Research, 62(12), 3383-3397.

[37]   Wiśniewski, R., & Blanke, M. (1999). Fully magnetic attitude control for spacecraft subject to gravity gradient. Automatica, 35(7), 1201-1214.

[38]   Zavoli, A., Giulietti, F., Avanzini, G., & De Matteis, G. (2016). Spacecraft dynamics under the action of Y-dot magnetic control law. Acta Astronautica, 122, 146-158.

[39]   Avanzini, G., de Angelis, E. L., & Giulietti, F. (2013). Acquisition of a desired pure-spin condition for a magnetically actuated spacecraft. Journal of Guidance, Control, and Dynamics, 36(6), 1816-1821.

[40]   Lukyanov D. P., Raspopov V. Y. and Filatov Yu. V. Basics of gyro theory. St. Petersburg. Concern CSRI Elektropribor, JSC, 2015, 316 p.

[41]   Gill, W. A., Howard, I., Mazhar, I., & McKee, K. (2022). A review of MEMS vibrating gyroscopes and their reliability issues in harsh environments. Sensors, 22(19), 7405.

[42]   Zhang, H., Zhang, C., Chen, J., & Li, A. (2022). A review of symmetric silicon MEMS gyroscope mode-matching technologies. Micromachines, 13(8), 1255.